Extended Abstracts of the 2007 International Conference on Solid State Devices and Materials, Tsukuba, 2007, pp. 906-907

C-7-1

Impacts of Cu/TaN Electrode on the Electrical Properties of Metal-insulator-metal $(Ba,Sr)TiO_3$ Thin-film Capacitors

Wen-Fa Wu[1,*], Kou-Chiang Tsai[1,2], Chuen-Guang Chao[2], Jain-Tsai Lee[2], Wei-Che Chang[3], Tsung-Kuei Kang[3], Guo-Shen Jheng[4], and Jian-Yang Lin[4]

[1] National Nano Device Laboratories, Hsinchu 30078, Taiwan, R.O.C.
Phone: +886-3-5726100-7715 E-mail: wfwu@mail.ndl.org.tw
[2] Department of Materials Science and Engineering, National Chiao-Tung University, Hsinchu, Taiwan, R.O.C.
[3] Department of Electronic Engineering, Feng-Chia University, Taichung, Taiwan, R.O.C.
[4] Department of Electronic Engineering, National Yunlin University of Science and Technology, Yunlin, Taiwan, R.O.C.

1. Introduction

The metal-insulator-metal (MIM) capacitors in silicon radio frequency (RF) and mixed-signal IC applications have recently attracted considerable attention, because they comprise highly conductive electrodes and have low parasitic capacitance [1]. The use of $(Ba,Sr)TiO_3$ (BST) in MIM capacitors has received increasing attention owing to its high dielectric constant, and excellent thermal and chemical stability. The electrodes are most important parts of such capacitors. Cu-based metallization technology can be incorporated into devices because of their ease of processing and the reduced production cost. However, Cu atoms can diffuse into Si devices, and their performance can be degraded by introducing deep level acceptors. Thus, effective diffusion barriers are required. Ta-based barriers have attracted the most attention owing to their high thermal stability and resistance to form compounds with copper [2]. In this study, the BST MIM capacitors with Cu-based electrodes were demonstrated. The maximum process temperature of 400ºC can fulfill the requirements of recently developed Cu and low-*k* interconnect technology. The fabrication of the devices is described and their characteristics are discussed as well.

2. Experiment

Test capacitors with an MIM structure were fabricated on SiO_2/Si substrates. Sputtered Ta/TaN layers were used to serve as barrier layers. Two Cu-based bottom electrode layers, Cu (300 nm) and TaN (25 nm)/Cu (300 nm) layers, were deposited by sputtering. The BST thin films of 70 nm thickness were deposited by sputtering a $Ba_{0.5}Sr_{0.5}TiO_3$ target at 400ºC. Table I lists the BST MIM capacitors utilized herein. BST-3 and BST-4 samples were annealed at 400ºC for 30 min in O_2 after BST films were deposited, to reduce the leakage current. Then, the 25nm TaN and 300nm Cu layers were sputtered as top electrodes.

The thickness of the film and the characteristics of its surface were measured by scanning electron microscopy. The samples were examined by cross-sectional transmission electron microscopy. Capacitances from 1 kHz to 1 MHz were measured using a Hewlett-Packard (HP4284A) precision *LCR* meter. Current density-electric field (*J–E*) characteristics were obtained using a HP4156B semiconductor parameter analyzer. During the electrical measurements, the top electrode was biased and the bottom electrode was grounded. The breakdown field (E_{bd}) was defined as the average applied field at which the current density through the dielectric exceeded $1\text{x}10^{-6}$ A/cm^2. Measurements of the time-dependence of dielectric breakdown (*TDDB*) were made at constant current stress to obtain about the traps in the BST.

Table I. Structures and thickness (nm) of BST MIM capacitors.

Type	Structures	Annealing
BST-1	Ta/TaN/Cu/BST/TaN/Cu	None
BST-2	Ta/TaN/Cu/TaN/BST/TaN/Cu	None
BST-3	Ta/TaN/Cu/BST/TaN/Cu	400°C, 30 min, O_2
BST-4	Ta/TaN/Cu/TaN/BST/TaN/Cu	400°C, 30 min, O_2

3. Results and Discussion

As presented in Fig. 1(a), the surface of the BST film in BST-3 sample is rough because it exhibits pinholes and hillocks, mostly of CuO, formed by oxidation at the BST/Cu electrode interface. The oxygen atoms from the environment easily penetrate the BST layer via diffusion paths and begin oxidizing the Cu layer. The surface of the BST-4 sample, as shown in Fig. 1(b), has almost no hillocks or pinholes. This study established that the TaN layer is impermeable to diffusing oxygen and so protects the underlying Cu layer against oxidation. The SEM observation is consistent with the TEM micrograph of the BST-4 sample, as shown in Fig. 2. The interface between the TaN and Cu layers is smoother and no reaction is observed between them.

Figure 3 plots the leakage current density as a function of electrical field up to 4.0 MV/cm. After annealing at 400°C for 30 min in O_2, the leakage current density of BST-3, not shown here, is caused by serious device failure due to Cu oxidation. However, the leakage current density of the BST-4 sample is $2.0\text{x}10^{-8}$ A/cm^2 at 1 MV/cm, significantly lower than that before annealing at 400°C. Also, the breakdown field (E_{bd}) of the BST-4 sample is around 3.2 MV/cm (at 10^{-6} A/cm^2), higher than those of the BST-1 and BST-2 samples, which are approximately 0.4 and 1.8 MV/cm. Post-annealing treatment in an oxygen-containing atmosphere yielded oxygen atoms and reduced the number of oxygen vacancies, ultimately enhancing the quality of BST films [3,4]. The time to breakdown (t_{BD}) of BST capacitors is measured by applying a voltage from 10.5 to 12.25 V, which corresponds to an electric field of 1.5 to 1.75 MV/cm in the BST-4 sample. Figure 4 plots log(t_{BD}) as a function of applied field. The BST-4 capacitor has a longer lifetime than 10 year at 1.1 MV/cm. This result indicates the long-term intrinsic reliability of the BST capacitor in Gbit-scale DRAM applications.

The capacitance density is maintained about 11.5 fF/μm^2 at frequency from 1 kHz to 1 MHz and a high dielectric constant of 91 is obtained, as shown in Fig. 5. The large capacitance density at a low frequency of 1 kHz, in combination with the decline in capacitance density at a high frequency of 1 MHz, reveals that the mechanism may be defect-related because the slow traps may not have sufficient speed to follow the high-frequency signals [5]. Furthermore, a low dissipation factor under 0.03 is observed. The dependence of capacitance on voltage can compared with the voltage coefficients of capacitance (VCCs), which are given by

$$dC/C_0 = \alpha V^2 + \beta V$$

where C_0 is the zero-biased capacitance at each frequency, and α and β are the quadratic and linear voltage coefficients, respectively. The capacitances are measured at 1 kHz, 10 kHz, 100 kHz and 1 MHz. Figures 6(a) and (b) plot the obtained α and β values. For BST-4 capacitor, α falls from 357 to 101 ppm/V^2 and β declines from 3637 to 1347 ppm/V. Both α and β decrease because the low time constant of traps within the BST layer and dipolar polarization diminished with increasing frequency. Furthermore, the presence of the interface effect can also contribute to the measured capacitance. Superior VCCs that suggest that the MIM capacitor is very useful in Si RF applications.

4. Conclusion

The BST MIM capacitor with Cu-based electrodes has a high capacitance density of 11.5 fF/μm^2 and a low dissipation factor below 0.03. It has a low leakage current density of 2.0×10^{-8} A/cm^2 and a high breakdown field of 3.2 MV/cm, small VCCs of 101 ppm/V^2, 1347 ppm/V, and a TDDB of over 10 years at 1.1 MV/cm. All these findings demonstrate that the BST MIM capacitors with Cu-based electrodes is very reliable in Gbit-scale DRAM applications, and is effective in silicon RF technology.

Reference

[1] C.H. Ng et al., IEEE Trans. Electron Devices 52(7) (2005) 1399.

[2] W.L. Yang et al., IEEE Trans. Electron Devices 49(11) (2002) 1947.

[3] D.E. Kotecki et al. IBM J. Res. Develop. 43(3) (1999) 367.

[4] J.W. Lee et al., J. Electrochem. Soc. 149(6) (2002) F56.

[5] M.Y. Yang et al., IEEE Electron Dev. Lett. 24(5) (2003) 306.

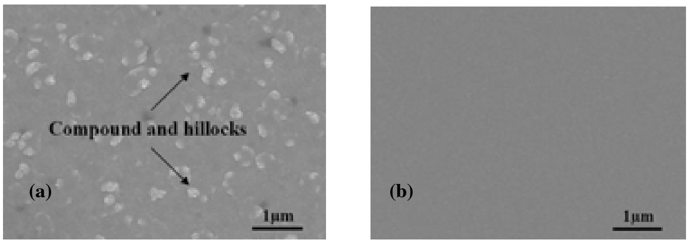

Fig. 1. SEM micrographs of BST films deposited on the (a) Cu and (b) TaN/Cu bottom electrodes after annealing at 400°C for 30 min in O_2.

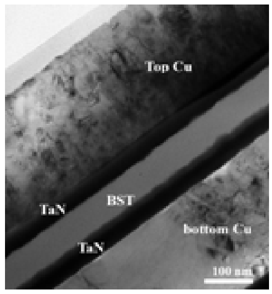

Fig. 2. Cross-sectional TEM image of the BST MIM capacitor with the Cu/TaN electrode..

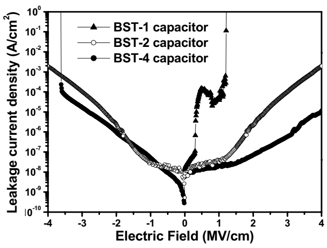

Fig. 3. *J-E* characteristics of BST MIM capacitors with various Cu-based electrodes after annealing at 400°C.

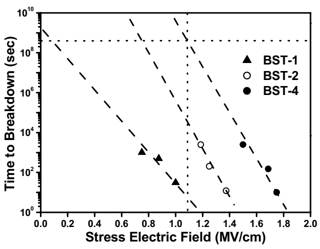

Fig. 4. Projected life-times of BST capacitors with Cu-based electrodes.

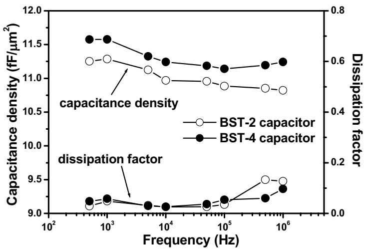

Fig. 5. Capacitance densities and dissipation factors of BST MIM capacitors as a function of frequency.

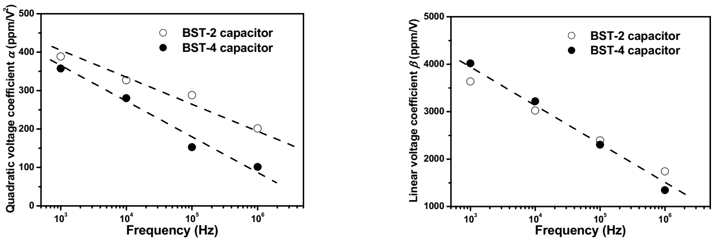

Fig. 6. (a) Quadratic voltage coefficients α and (b) linear voltage coefficients β of capacitances of BST-4 capacitors with Cu/TaN electrodes as a function of frequency.